PCCP

Accepted Manuscript

ROYAL SOCIETY OF CHEMISTRY

www.rsc.org/pccp

Revised version for PCCP, 2014-8-12

State-to-State Dynamics of high-*n* Rydberg H-atom Scattering with H_2: Inelastic Scattering and Reactive Scattering

Shengrui Yu, Shu Su, Dongxu Dai, Kaijun Yuan*, Xueming Yang*

State key Laboratory of Molecular Reaction Dynamics, Dalian Institute of Chemical Physics, Chinese Academy of Sciences, 457 Zhongshan Road Dalian 116023, China

** To whom correspondence should be addressed. Email addresses: kjyuan@dicp.ac.cn, xmyang@dicp.ac.cn*

Abstract

The state-to-state dynamics of high-*n* Rydberg H-atom scattering with *para*-H_2 at the collision energies of 0.45 and 1.07 eV have been carried out using H-atom Rydberg tagging time-of-flight technique. Both the inelastic scattering and reactive scattering are observed in the experimental time-of-flight spectra. The products H_2 (v', j'=odd) only come from reactive scattering and present clearly forward-backward asymmetric angular distributions, which differ from that of the corresponding ion-molecule reaction. The products H_2 (v', j'=even), however, come from both reactive scattering and inelastic scattering. Simulating the rotational distribution from reactive scattering, we found most of H_2 (v', j'=even) products come from inelastic scattering. The angular distributions of the product H_2 (v', j'=even) are consistent with what is predicted by the conventional textbook mechanism of inelastic scattering, and are a little different from that of the corresponding ion-molecule inelastic scattering. These results suggest that the effect of Rydberg electron could not be neglected in describing the differential cross sections of H* + *para*-H_2 scattering. From the simulation, the branching ratios of inelastic scattering channel were determined to be 66% and 79% at the collision energies of 0.45 and 1.07eV, respectively.

1. Introduction

Collisions between Rydberg atoms (RA) and neutral molecules are a curious type of collision, which do not follow the same dynamics as those involving ground state or low-lying excited state species.[1,2,3,4] Because the electron in a high Rydberg state spends most of its time far from the ion core, it is often physically reasonable to describe such collision processes theoretically by the independent-collider model,[5] in which electron-target and ion core-target scattering events are treated independently. This model of RA collisions was originally proposed by Fermi, and has been used to interpret a wide range of Rydberg state collision phenomena.[6,7,8,9]

Over the last few decades, the collision processes of highly excited RAs have been the subject of intense study.[10] To date, however, rather little work has been done on full quantum-state resolved RA collisions. Davis and co-workers[11] first studied vibrationally resolved inelastic scattering of H-RA with N_2 and O_2 at the collision energy of 1.84 eV by the H-atom Rydberg tagging time-of-flight (HRTOF) technique. Their results confirmed that the inelastic collisions of these systems resemble closely the corresponding ion-molecule scattering. Recently, Yu *et al.* reinvestigated the typical inelastic collision of H-RA with O_2 at two lower collision energies of 0.64 and 1.55 eV.[12] The striking phenomenon observed in this work was the extremely high vibrational excitation of O_2 products in the backward-scattered direction, which was explained by a double charge transfer mechanism suggested by Gianturco *et al.* in an early study of $H^+ + O_2$ collision.[13] This finding was a further illustration that the Fermi independent-collider model may be applied to RA inelastic collisions with

nonpolar molecules at a fully state resolved level.

In addition to RA-molecule inelastic scattering, chemically reactive collisions involving RAs have also attracted much attention in the past few years. Recently, the dynamics of RA reactive scattering H*(n) + o-D_2 → HD + D*(n') has been studied experimentally by means of the HRTOF technique by Yang *et al.*[14,15] and by Wrede *et al*.,[16] respectively. In those experiments, the rotationally resolved product distribution measured for the RA-molecule reaction at a single scattering angle reproduced the experimental product distribution of the corresponding $H^+ + D_2 \rightarrow HD + D^+$ reaction. A practical application of these works is that RAs may be useful for studies of elementary ion-molecule reactions. Subsequently, motivated for this principal finding, comparisons with theoretical results of $H^+ + D_2$ collision obtained in exact quantum mechanical and quasiclassical trajectory calculations were extensively reported.[17,18,19] However, full angular, quantum-state resolved differential cross-sections (DCSs) of the H* + o-D_2 reaction obtained firstly by Yu *et al*.[20] showed that the angular distributions of HD product rotational states presented a strong preference for forward scattering, which were obviously different from those of corresponding ion-molecule reactions. Such marked difference suggests that Fermi independent-collider model is not valid in describing the DCSs of RA reactions with molecules. A similar conclusion has also been obtained in a recent study of H*(n) + HD → D*(n') + H_2 reactive scattering by Yu *et al*.[21] These studies remind us that, unlike RA inelastic scattering, caution should be exercised when testing theoretical methods performed for ionic systems with the measurements carried out in reactions with RAs.

Although a vast amount of data is available from the collisions between H-RA and molecules, the detailed information regarding an H-RA collision process to produce the inelastically scattered products and reactively scattered products is still not well understood. To our knowledge, in order to obtain a more complete picture of the inherent dynamics of one collision system, the data of inelastic scattering and reactive scattering are both indispensable. In the present work, the prototypic collision of H-RA with *para*-H_2 was experimentally investigated at the collision energies of 0.45 eV and 1.07 eV using the H-atom Rydberg tagging time-of-flight technique to characterize inelastic and reactive channels involving this scattering, simultaneously.

2. Experimental Methods

In this work, full quantum-state resolved crossed beam scattering of the highly excited Rydberg H atom with *para*-H_2 has been carried out using the crossed molecular beam apparatus with H-atom Rydberg "tagging" technique.[22,23,24,25] Detailed of this experimental setup used for studying inelastic and/or reactive scattering of Rydberg H atom with neutral molecule has been described previously. [20] Briefly, two parallel molecular beams (HI and *para*-H_2) are generated by pulsed valves. The *para*-H_2 beam is produced by an adiabatic expansion through a nozzle cooled to the liquid nitrogen temperature, which ensures that almost all molecules in the beam are in the H_2 (v=0, j=0) state with a reduced velocity spread. The cooled *para*-H_2 beam has a velocity of 1380 m/s with a speed ratio ($\upsilon/\Delta\upsilon$) of about 25 in this work. The H-RA beam at a high Rydberg level (n=~46) is created through pumping the H atoms produced from photodissociation of HI molecules at 266 nm to a high-n

Rydberg state via resonant two-photon excitation using two excitation laser beams of 121.6 and 365.8 nm wavelength at about 5 mm away from the scattering region. The polarization direction of the 266 nm is chosen to direct the slow (or fast) H atoms corresponding to the formation of iodine atoms in their spin orbit excited state (or ground state). The H-RA beam with the nascent velocity of the H atom products (11230 or 17470 m/s) then crosses perpendicularly with the *para*-H_2 beam. After traversing a certain TOF distance, the scattered H-RAs which remain in the high-*n* Rydberg states ($n \geq 20$) are readily detected by field ionization in a rotating MCP detector. In this work, both the inelastically scattered H-RAs [$\boldsymbol{H}^*(n=46) + H_2(v=0, j=0) \rightarrow \boldsymbol{H}^*(n') + H_2(v', j')$, eqn (1)] and reactively scattered H-RAs [$\boldsymbol{H}^*(n=46) + H_2(v=0, j=0) \rightarrow H^*(n') + H\boldsymbol{H}(v', j')$, eqn (2)] could be recorded, but no ionizing processes are detectable because all ion signals from the collision region are pulled away by applying an external electric field (~20V/cm). Furthermore, in an effort to measure complete angular distribution by the rotating MCP detector in this experiment, a liquid nitrogen cooled copper block is installed downstream of the HI molecular beam. This copper block could significantly eliminate the attenuation of the scattering signals in the forward directions ($\theta_{Lab} < -40°$) through absorbing the HI beam during scattering.

3. Results and Discussions

3.1. $\boldsymbol{H}^*(n) + H_2(v=0, j=0) \rightarrow H^*(n') + H\boldsymbol{H}(v', j')$ reactive scattering

TOF spectra of the scattered H-RA products from elastic/inelastic scattering and

reactive scattering have been measured at 17 laboratory scattering angles (from 85° to −70° at about 10° interval) using HRTOF technique described above. The direction of the *p*-H_2 beam is defined as θ_{Lab} = 0°, while the direction of the H-RA beam is at θ_{Lab} = 90°. These TOF spectra can be converted to the velocity spectra using a standard Jacobian transformation from the laboratory (LAB) frame to the center-of-mass (CM) frame. Figure 1 illustrates three velocity spectra of the scattered H-RA products at the collision energy of 0.45eV, which correspond to the forward (θ_{Lab} = -50°), sideway (θ_{Lab} = 30°), and backward (θ_{Lab} = 85°) collision directions in the CM frame. It is quite clear that these spectra consist of a series of sharp structures, which can be unambiguously assigned to the different rotationally excited H_2 (v'=0, j'=0-7) products. It is necessary to point out that the inelastic process (eqn (1)) and reactive process (eqn (2)) have similar reaction enthalpy and produced species, Thus, the source of H_2 products cannot be able to distinguish at once based on those velocity distributions. However, as noted in the previous studies, [14,21,26] the *ortho-para* transitions are forbidden in inelastic collisions. As for H*+*p*-H_2 collision, the odd H_2 rotational levels should be not populated in the ***H****(n) + *para*-H_2 → ***H****(n') + H_2(v', j') inelastic scattering. Therefore, the odd-j' scattered H_2 products should be only from the ***H****(n) + *para*-H_2 → H*(n') + H***H***(v', j') reactive scattering, while the even-j' scattered H_2 products come from both two scattering processes.

Figure 2 shows three velocity spectra at high collision energy of 1.07eV, which also correspond to the forward (θ_{Lab} = -50°), sideway (θ_{Lab} = 30°), and backward (θ_{Lab} = 85°) collision directions in the CM frame. One marked difference from that in the 0.45 eV collision is more sharp peaks are observed, which can be assigned to the different rotational states of H_2 products with vibrational excitation at v=0 and 1. Such phenomenon is consistent to the fact that more available energy will be

deposited into the products with high (v', j') values as the collision energy increases.

The velocity spectra obtained experimentally in the LAB frame are simulated by adjusting the relative populations of the rovibrational states of the H_2 products. From these fits, relative populations of H_2 products at different rovibrational states were determined at 17 LAB angles. State-resolved distributions of the H_2 products in the CM frame were then determined by a polynomial fit to the above results, and from these distributions, state-resolved DCSs were determined. By incorporating all of the velocity distribution in the CM frame, a three-dimensional (3D) contour plot of the DCSs was constructed. Figure 3 shows such DCSs for H-RA products from the $\boldsymbol{H}^*(n)$ + H_2 (v'=0, j'=0) → H*(n') + H$\boldsymbol{H}$(v', j'=odd) reactive scattering at the collision energies of 0.45 and 1.07eV. The forward-scattering direction for H-RA products from the reactive scattering is defined along the indicated arrow corresponding to the direction for the *para*-H_2 molecular beam. The state-resolved angular distributions for the $\boldsymbol{H}^*(n)$ + H_2 (v'=0, j'=0)→ H*(n') + H$\boldsymbol{H}$(v', j'=odd) reactive scattering at the collision energies of 0.45 and 1.07eV were plotted in Figure 4. From Figure 3 and 4, the remarkable feature is the extremely peaked character in both forward and backward scattering directions. In particular, the ratio of DCSs between extreme forward and sideways is more than 10, for the lowest j′ values. Considering our experimental detection method, the actual ratio of DCSs between extreme forward and sideways would be much larger. (Due to the limited angular resolution of the MCP detector, the signal would be average over 3~5^o, which means the peak intensity detected around 180^o or 0^o is much lower than the actual value.) Such features have been observed in the corresponding ion-molecule reaction H^++H_2 by Lezana et al[27]. This extreme polarization effects between forward/backward and sideway scattering has only been reproduced by the QM methods. The QCT DCS, on the contrary,

cannot reproduce the extreme forward and backward scattering. Such phenomenon has also been found in some insertion reactions such as $C(^1D)+H_2$[28], $S(^1D)+H_2$[29], and $O(^1D)+HD$[30].

Another interesting feature is that the structure of the rotational resolved DCS shows a strong dependence on the specific value of j′. For j′=1 and 3, forward scattering is preferred, while for j′=7, backward scattering is preferred. This feature is more pronounced for v′=0 and 1 products at high collision energy of 1.07eV. Though the rotationally resolved DCSs for the ***H****(n) + H_2 (v'=0, j'=0)→ H*(n') + H***H***(v', j'=even) could not be obtained, the propensity of DCSs for H***H***(v', j'=even) should be similar with that of H***H***(v', j'=odd), as reported in the previous studies of isotopic variants, H* + *o*-D_2[20], H* + HD[21] collision. This means the total DCS for the ***H****(n) + H_2 (v'=0, j'=0) → H*(n') + H***H***(v', j') should be forward scattered, which is different from that reported by Lezana *et al.* in the corresponding ion-molecule reaction H^++H_2. They obtained the roughly forward-backward symmetric total DCS arising from the formation of a long lived collision complex H_3^+. The breakdown of this symmetry in RA reactive scattering, especially favouring forward scattering, may be interpreted in terms of the osculating complex model as a reduction of the complex lifetime below its rotational period. Indeed, the quantum number of the Rydberg H* atom could be changing during the exchange reaction. Thus, the Rydberg electron with different orbit periods may affect the lifetime of the intermediate complex. Far more detailed experimental and theoretical studies are necessary to clarify this hypothesis.

Total quantum state distributions are also determined by integrating those DCSs over different CM angles. Figure 5 shows the H_2 rotational distributions for ***H****(n) + *para*-H_2 → H*(n') + H***H***(v', j') reactive scattering at the collision energies of 0.45 and 1.07eV, respectively. From those distributions, it is difficult to separate the

contribution from inelastic scattering and reactive scattering immediately, since the signals from inelastic and reactive scattering overlap with each other for the $H_2(v', j'$=even) products. Fortunately, according to the previous studies, the total product rotational distributions from H-RA reactive scattering should exhibit statistical-like distribution[20,21], and the total product rotational distributions from H-RA reactive scattering are quite similar with that from the corresponding ion-molecule reaction. Theoretical study for $\mathbf{H}^+ + H_2 \rightarrow H^+ + H\mathbf{H}$ reaction also showed statistical-like product rotational distributions[27,31]. Thus, we can obtain the statistical-like artificial rotation distributions based on the experimental odd-j' population, as shown in Figure 6. From those new distributions, it is interesting to find that the rotational distribution for vibrationally excited $H_2(v'=1)$ products at high collision energy is striking hot with the intensive peak of $j'=7$ near its energetic limit, whereas the rotational distributions for ground vibrational $H_2(v'=0)$ products is moderate at both two collision energies.

3.2. $H^*(n=46) + H_2(v=0, j=0) \rightarrow H^*(n') + H_2(v', j'$=even) inelastic scattering

In this study, we also can obtain the H-RA inelastic scattering dynamics. As discussed above, the even-j' scattered H_2 products come from both inelastic scattering and reactive scattering processes. From Figure 5 and 6, it is clear that the signals from H-RA inelastic scattering are much larger than that from H-RA reactive scattering. About 20.5% and 10.4% even-j' H_2 products come from reactive channel at the collision energies of 0.45 and 1.07eV, respectively. Subtracting the reactive component simulated in Figure 6, We can get the rotational distributions of the $H_2(v'$, j'=even) products from inelastic scattering at the collision energies of 0.45 and 1.07eV.

As can be seen from Figure 7, the relative intensity of H_2 (v'=0) rotational excited states decrease monotonously as rotational energy increases at both two collision energies, indicating that rotational excitation is quite cold. However, the vibrationally excited H_2 (v'=1) products from high collision energy appear to be moderate rotational excitation, with the peak at j'=4. This is reasonable since vibrationally excited H_2 products come from the collisions with small impact parameters. Such collisions usually can transfer large angular force. Integrating the reactive scattering and the inelastic scattering, the branching ratios of inelastic scattering channel (eqn (1)) were determined to be 66% and 79% at the collision energies of 0.45 and 1.07eV, respectively. During the fitting, we used an assumption that the rotational distribution from reactive scattering is statistical. The fitting error bars are estimated to be ±10%. It seems that the contribution from inelastic scattering is relatively larger at higher collision energy.

The 3D contour plots of the DCSs and state-resolved angular distributions for H-RA products from H*(n) + H_2 (v=0, j=0) → H*(n') + H_2 (v', j'=even) at the collision energies of 0.45 and 1.07 eV are displayed in Figure 8 and 9, respectively. Based on the analysis above, these results cannot exactly present the dynamics of H_2 (v', j'=even) products from H-RA inelastic scattering, but would be quite similar with the real results. It is interesting that the distributions show a strong dependence on the specific rovibrational states. The low rotationally excited H_2 products (j'=0, 2) are mostly forward-scattered, whereas for highly rotationally excited H_2 products (j'=4, 6), the DCSs become nearly backward-scattered with some extent of forward-scattered. Such

change is much more significant at the collision energy of 1.07 eV, in which the DCSs for H_2 at v'=1 is clearly backward-scattered. The experimental observations are exactly consistent with what is predicted by the conventional textbook mechanism,[32] in which collisions with high impact parameters are forward-scattered and essentially low energy transfer from kinetic energy to rovibrational energy, whereas collisions with low impact parameters transfer a large amount of energy into rovibrations and are mainly backward-scattered. Such observation is a little different with the inelastic scattering from the corresponding ion-molecule scattering. Anomalously forward scattering in vibrational inelastic collision has been observed in scattering of H^+ with H_2, HD and D_2 reported by Giese *et al.* [33]. They suggested a different mechanism in which the passing proton withdraws electron density from the diatomic target, stretches the bond of target molecule and inducing vibrational excitation. Anomalously forward scattering has also been observed in vibrationally inelastic $H+D_2$ collisions studied by Greaves and coworkers[34,35], in which they observed the D_2 products are dominantly forward-scattered at all vibrational excited states, and attributed such phenomenon to strong attractive forces when H atom moves close to D_2 molecule. It is clear that H-RA inelastic scattering presented here is different with the ion inelastic scattering H^++H_2 and also different with the ground H inelastic scattering $H+D_2$. The possible reason is Rydberg electron has effect on the differential cross section of H-RA inelastic scattering. This means Fermi independent-collider model is also not valid in describing the DCSs of H-RA inelastic collision with molecules.

□ Conclusion

In this work, the state-to-state dynamics of high-*n* Rydberg H-atom scattering with *para*-H_2 have been investigated using the HRTOF method at the collision energies of 0.45 and 1.07 eV. Rotational distribution and angular distribution of H_2 product have been presented. The H_2 (v', j'=odd) products, which come from reactive scattering, present a strong preference for forward scattering. Such propensity is also observed in the previous works on H-RA reaction with D_2 and HD, but different with that of the corresponding ion-molecule reaction. The H_2 (v', j'=even) products, which dominantly come from inelastic scattering, show forward scattering at low rotational states and backward scattering at high rotational states. This is consistent with what is predicted by the conventional textbook mechanism of inelastic scattering. By simulating the rotational distribution from reactive scattering, the branching ratios of inelastic scattering channel were determined to be 66% and 79% at the collision energies of 0.45 and 1.07eV, respectively. The present study of the H* + *para*-H_2 collision provide us deep insight into this interesting H-RA scattering process.

Acknowledgments

We are very grateful for the support of this work by the National Natural Science Foundation of China (No.21103185, No. 2013CB834604), the Chinese Academy of Sciences and the Ministry of Science and Technology.

Figures and Captions

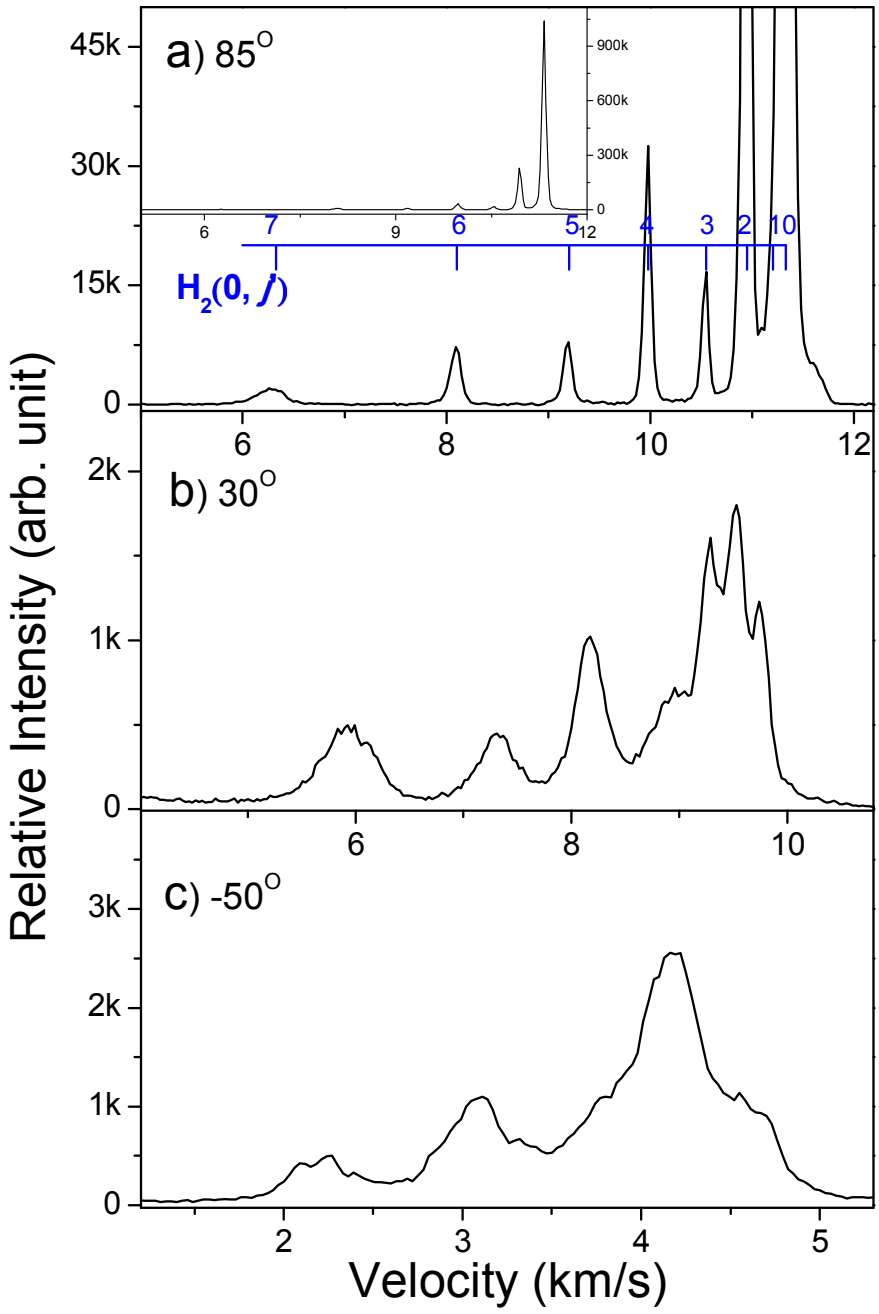

Fig. 1 Velocity spectra of the scattered H-RA products from the H*(n=46) + H_2(v=0, j=0) scattering at three typical laboratory angles of 85°(a), 30°(b), -50°(c) off the *para*-H_2 beam at the collision energy of 0.45eV.

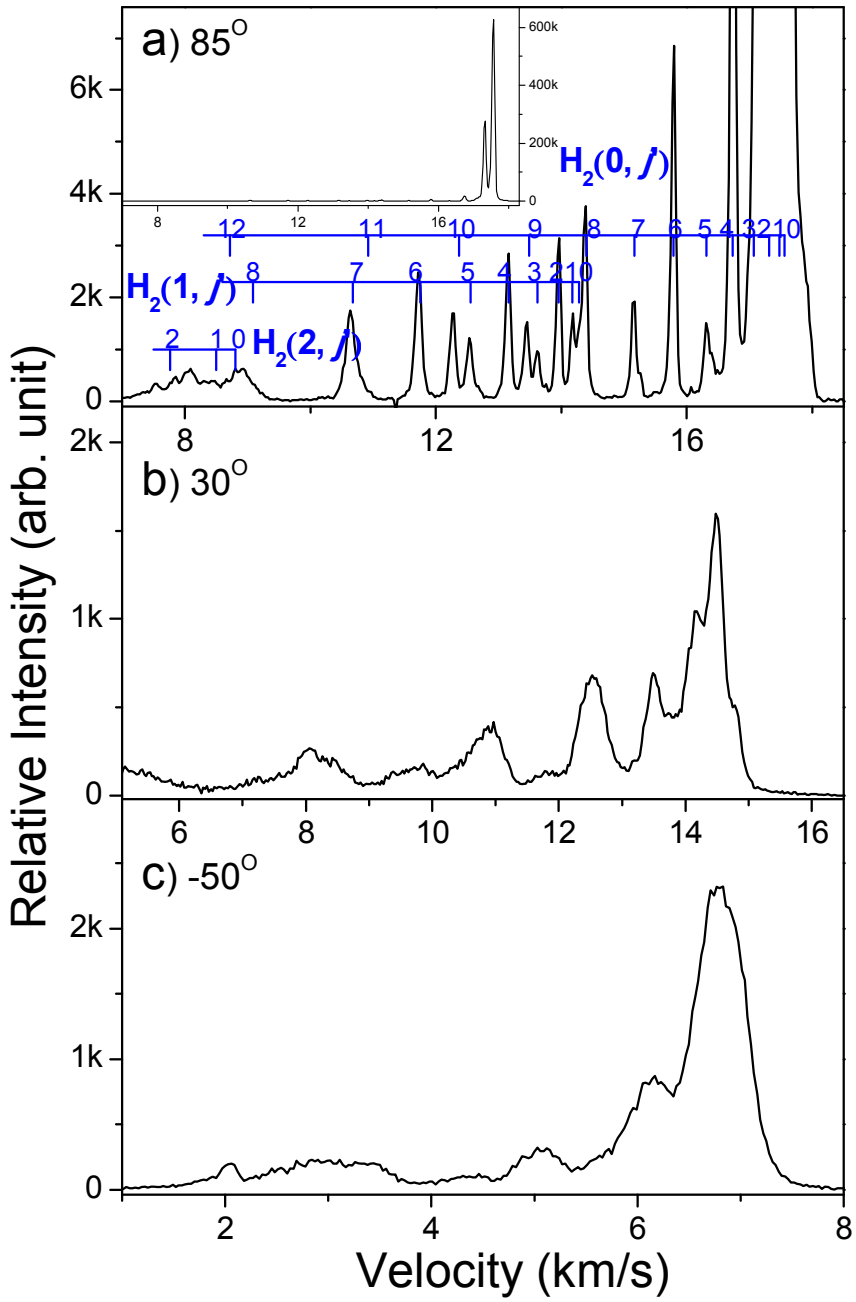

Fig. 2 Velocity spectra of the scattered H-RA products from the H*(n=46) + H_2(v=0, j=0) scattering at three typical laboratory angles of 85°(a), 30°(b), -50°(c) off the *para*-H_2 beam at the collision energy of 1.07eV.

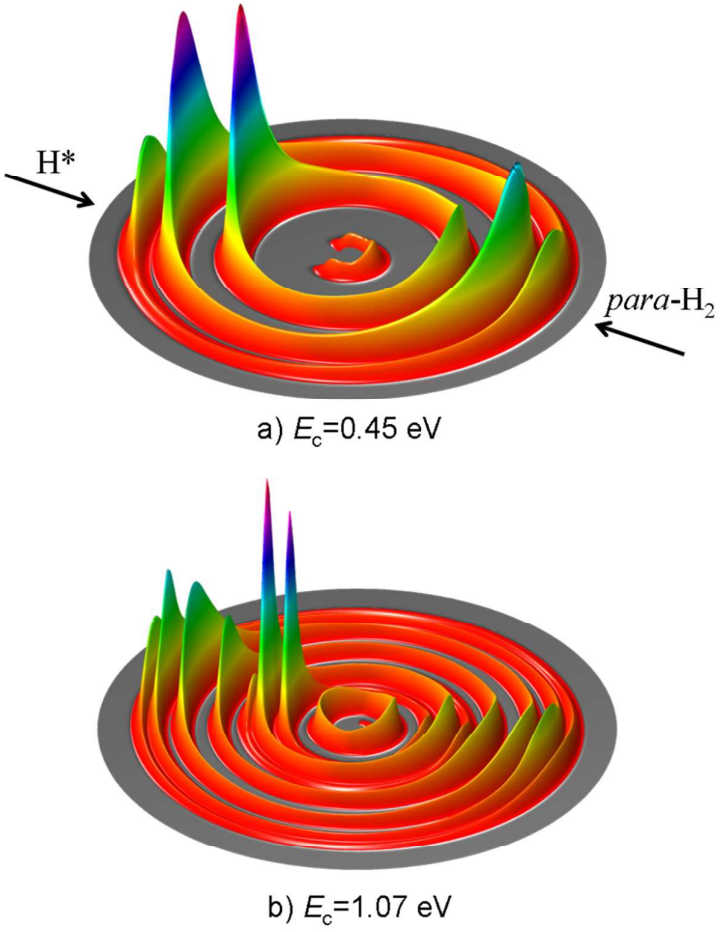

Fig. 3 The experimental 3D contour plots of the DCSs for the H-RA products from ***H****(n=46) + H_2(v=0, j=0) → H*(n') + H***H***(v', j'=odd) reaction at the collision energies of 0.45 (a) and 1.07 eV (b).

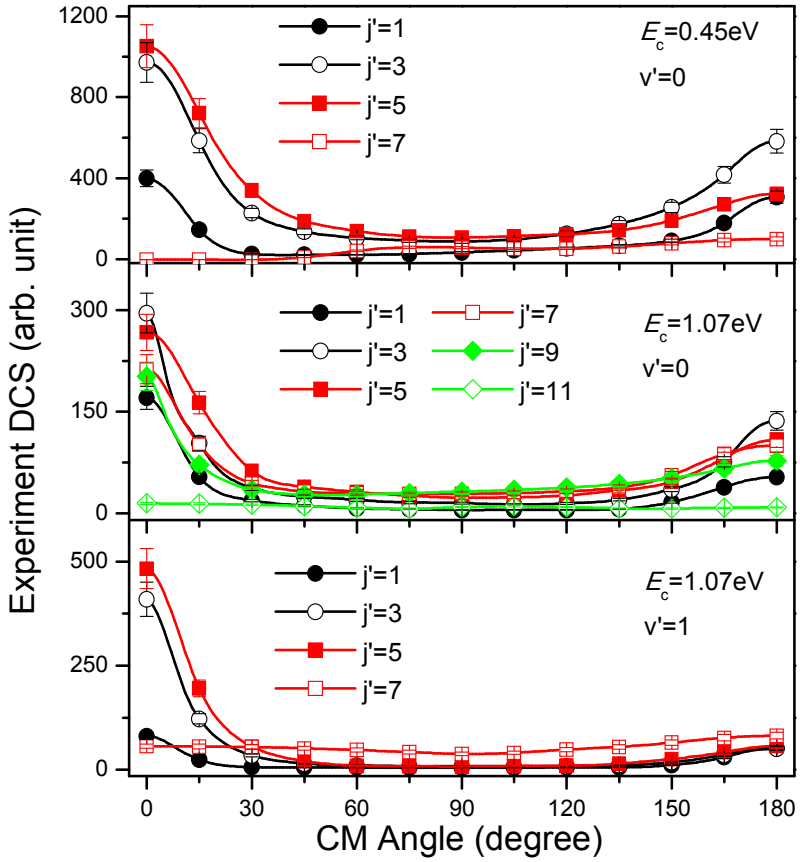

Fig. 4 The rotational state-resolved angular distributions of H_2 (v', j'=odd) products from reactive scattering at the collision energies of 0.45 and 1.07eV.

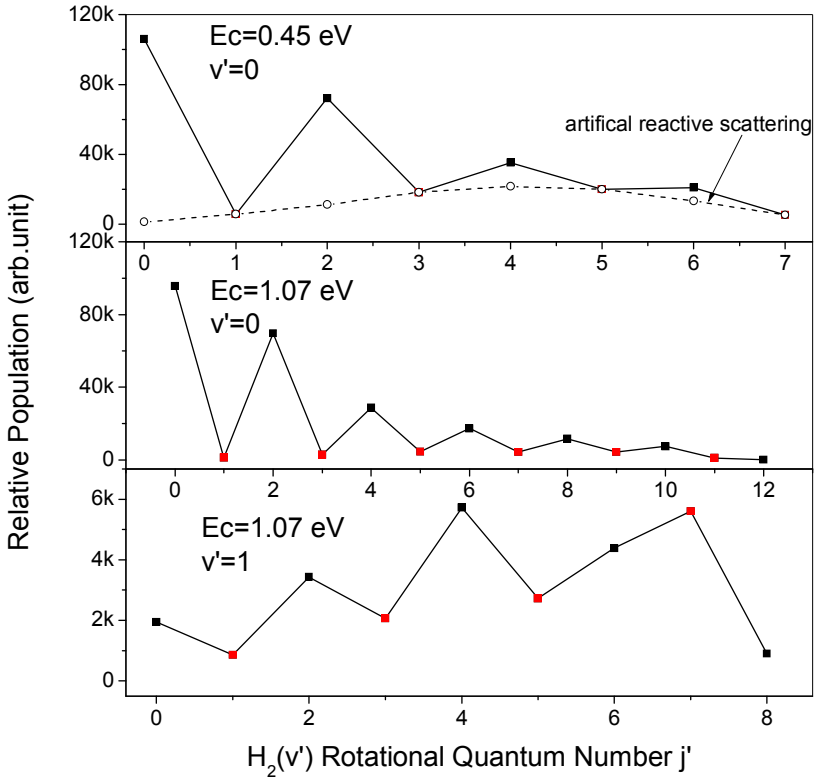

Fig. 5 Rotational distributions of the H_2 (v', j') products for the H*(n=46)+H_2(v=0, j=0) →H_2(v', j') +H* reaction at E_{coll}=0.45 eV and 1.07 eV.

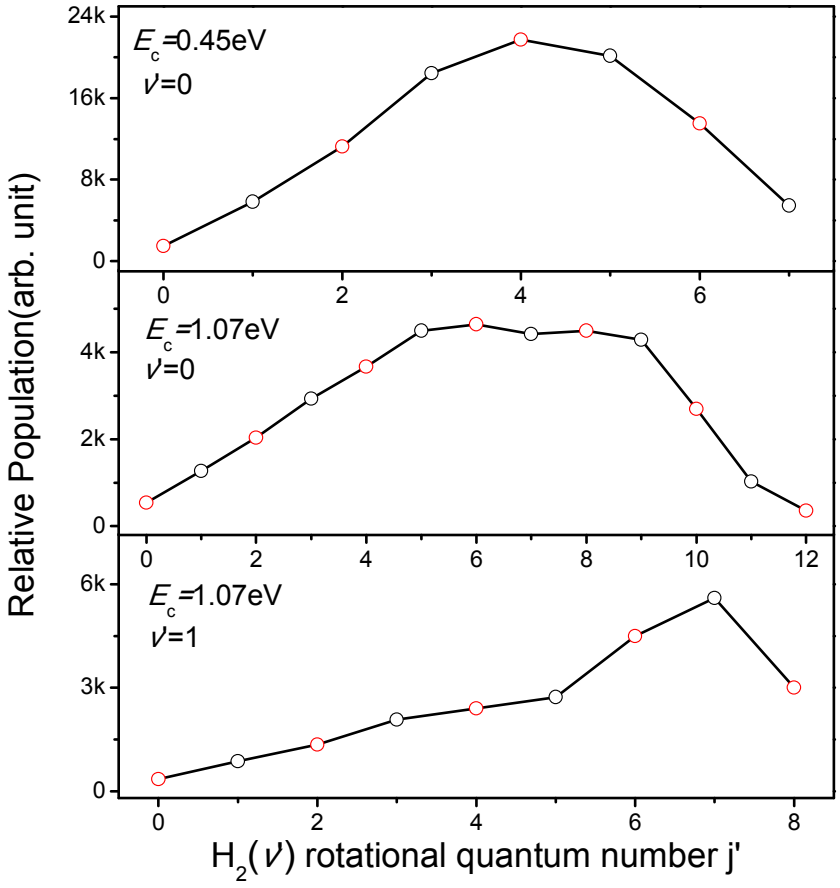

Fig. 6 Rotational distributions of the H_2 products for the ***H****(n=46) + H_2(v=0, j=0) → H*(n') + H***H***(v', j') reaction at the collision energies of 0.45 and 1.07 eV. The black circles are the experimental data for ***H****(n=46) + H_2 (v=0, j=0) → H*(n') + H***H***(v', j'=odd) reaction. The red circles are the (artificial) distributions using Boltzmann statistics distribution.

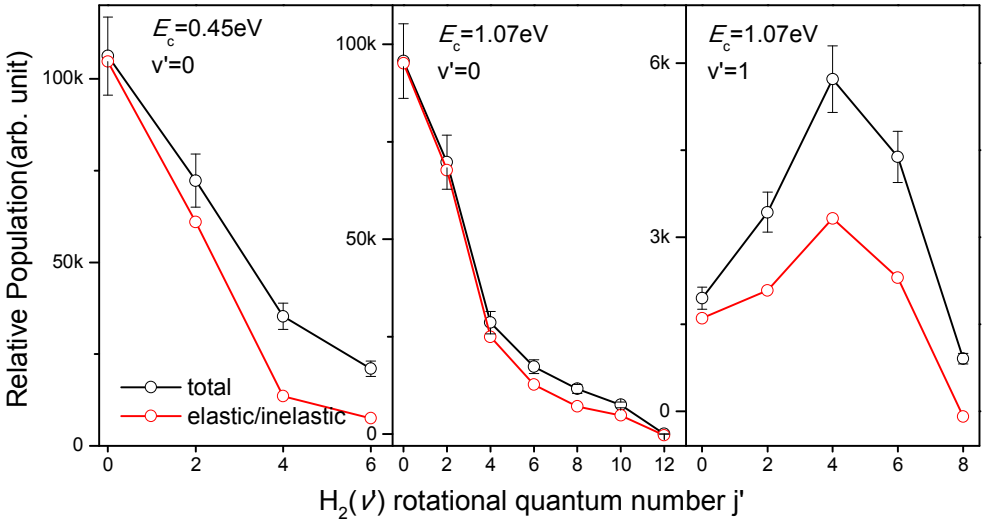

Fig. 7 Rotational distributions of the $H_2(v', j'$=even) products at the collision energies of 0.45 and 1.07 eV. The black lines are the experimental results of H*(n=46) + $H_2(v$=0, j=0) → H(n') + $H_2(v', j'$=even) collision. The red lines are the distributions for **H***(n=46) + *para*-H_2 → **H***(n') + $H_2(v', j')$ collision by subtracting the reactive component simulated in Figure 6.

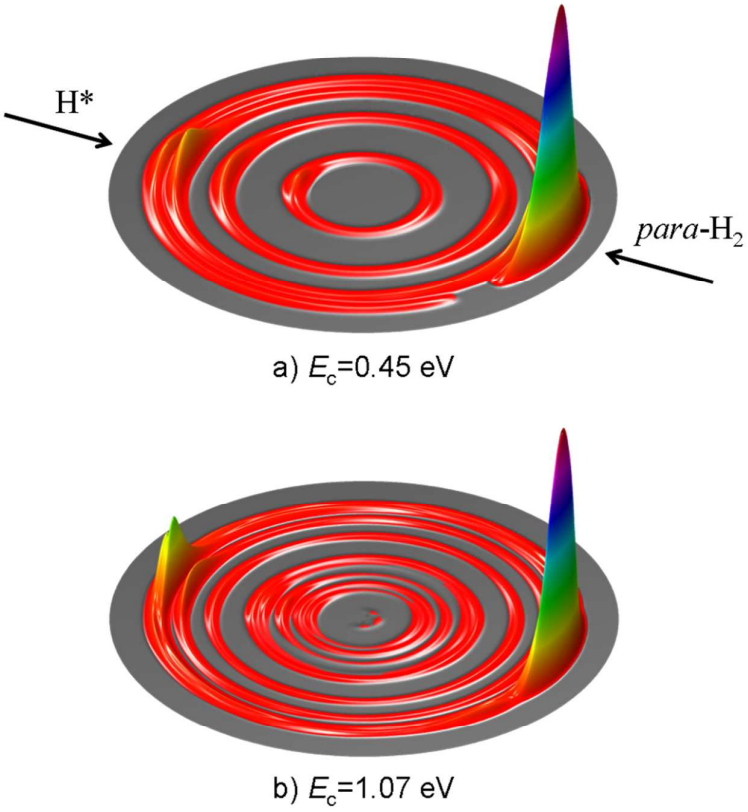

Fig. 8 The experimental 3D contour plots of the DCSs for the H-RA products from $H(n=46) + H_2(v=0, j=0) \rightarrow H(n') + H_2(v', j'=\text{even})$ collision at the collision energies of 0.45 (a) and 1.07 eV (b).

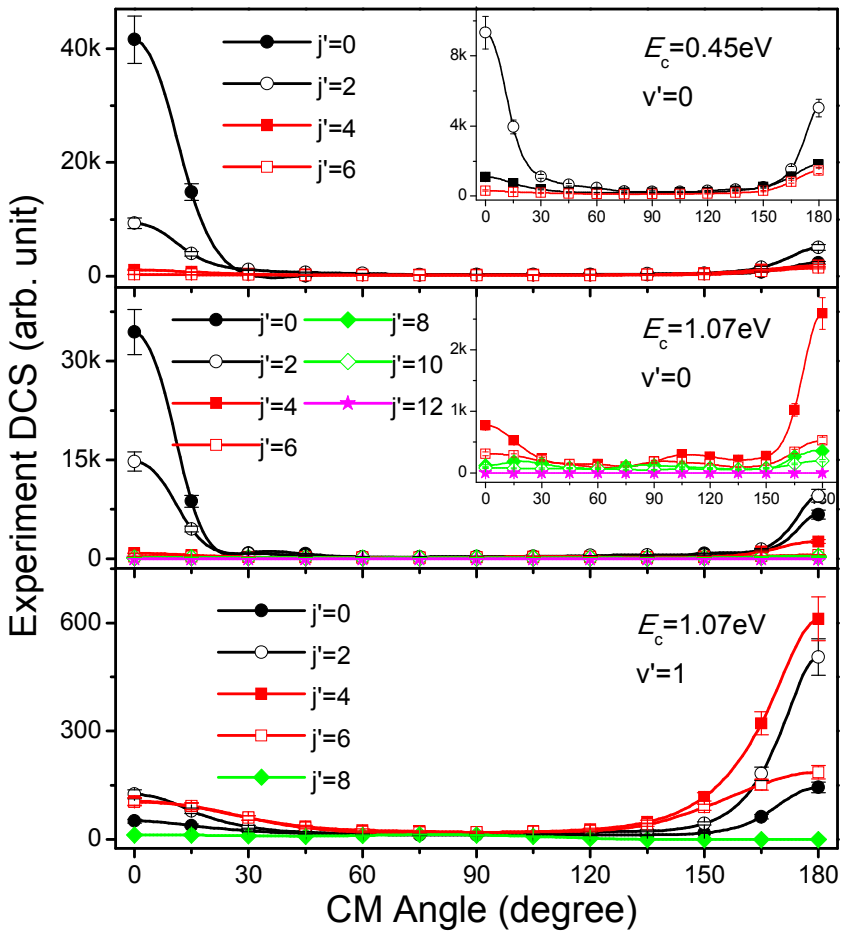

Fig. 9 The state-resolved angular distributions of $H_2(v', j'$=even) products from both reactive scattering and elastic/inelastic scattering at the collision energies of 0.45 and 1.07eV.

Reference

[1] M. Matsuzawa, in *Rydberg State of Atoms and Molecules*, ed. R. F. Stebbings and F. B. Dunning, Cambridge University Press, New York, 1983.

[2] F. B. Dunning and R. F. Stebbings, *Annu. Rev. Phys. Chem.* 1982, **33**, 173-189.

[3] T. F. Gallagher, *Rydberg Atoms*, Cambridge University Press, Cambridge, 1994.

[4] J. Jankunas, R. N. Zare, F. Bouakline, S. C. Althorpe, D.Herráez-Aguilar and F. J. Aoiz, *Science*, 2012, **336**, 1687-1690.

[5] E. Fermi, *Nuovo Cimento* 1934, **11**, 157-166.

[6] P. M. Koch, *Phys. Rev. Lett.* 1979, **43**, 432-435.

[7] L. J. Wang, M. King and T. J. Morgan, *J. Phys. B: At. Mol. Opt. Phys.* 1986, **19**, L623- L628.

[8] B. S. Strazisar, C. Lin and H. F. Davis, *Phys. Rev. Lett.* 2001, **86**, 3997-4000.

[9] S. T. Pratt, J. L. Dehmer and P. M. Dehmer, *J. Chem. Phys.* 1994, **101**, 882-890.

[10] R. F. Stebbings and F. B. Dunning, *Rydberg State of Atoms and Molecules*, Cambridge University Press, New York, 1983.

[11] B. S. Strazisar, C. Lin and H. F. Davis, *Phys. Rev. Lett.* 2001, **86**, 3997-4000.

[12] S. R. Yu, S. Shu, K. J. Yuan, D. X. Dai and X. M. Yang, *J. Phys. Chem. Lett.* 2012, **3**, 2420-2424.

[13] F. A. Gianturco, U. Gierz and J. P. Toennies, *J. Phys. B: At., Mol. Opt. Phys.* 1981, **14**, 667-677.

[14] D. X. Dai, C. C. Wang, G. R. Wu, S. A. Harich, H. Song, M. Hayes, R. T. Skodje, X. Y. Wang, D. Gerlich and X. M. Yang, *Phys. Rev. Lett.* 2005, **95**, 013201.

[15] H. Song, D. X. Dai, G. R. Wu, C. C. Wang, S. A. Harich, M. Y. Hayes, X. Y. Wang, D. Gerlich, X. M. Yang and R. T. Skodje, *J. Chem. Phys.* 2005, **123**, 074314.

[16] E. Wrede, L. Schnieder, K. Seekamp-Schnieder, B. Niederjohann and K. H. Welge, *Phys. Chem. Chem. Phys.* 2005, **7**, 1577-1582.

[17] E. Carmona-Novillo, T. González-Lezana, O. Roncero, P. Honvault, J.-M. Launay, N. Bulut, F. J. Aoiz, L. Bañares, A. Trottier and E. Wrede, *J. Chem. Phys.* 2008, **128**, 014304.

[18] T. González-Lenzana, P. Honvault, P. G. Jambrina, F. J. Aoiz and J.-M. Launay, *J. Chem. Phys.* 2009, **131**, 044315.

[19] P. G. Jambrina, F. J. Aoiz, N. Bulut, S. C. Smith, G. G. Balint-Kurti and M. Hankel, *Phys. Chem. Chem. Phys.* 2010, **12**, 1102-1115.

[20] S. R. Yu, K. J. Yuan, H. Song, X. Xu, D. X. Dai, D. H. Zhang and X. M. Yang, *Chem. Sci.* 2012, **3**, 2839-2842.

[21] S. R. Yu, S. Su, D. X. Dai, K. J. Yuan and X. M. Yang, *J. Chem. Phys.* 2014, **140**, 034310.

[22] L. Schnieder, W. Meier, E. Wrede, K. H. Welge, M. N. R. Ashfold and C. M. Western, *J. Chem. Phys.* 1990, **92**, 7027-7037.

[23] L. Schnieder, K. Seekamp-Rahn, E. Wrede and K. H. Welge, *J. Chem. Phys.* 1997, **107**, 6175-6195.

[24] K. J. Yuan, L. N. Cheng, Y. Cheng, Q. Guo, D. X. Dai and X. M. Yang, *Rev. .Sci. Instrum.* 2008**, 79**, 124101.

[25] K. J. Yuan, Y. Cheng, L. N. Cheng, Q. Guo, D. X. Dai, X. Y. Wang, X. M. Yang and R. N. Dixon, *Proc. Natl. Acad. Sci. U.S.A.* 2008**, 105**, 19148-19153.

[26] M. Faubel and G. Kraft, *J. Chem. Phys.* 1986, **85**, 2671-2683.

[27] T. González-Lezana, O. Roncero, P. Honvault, J.-M. Launay, N. Bulut, F. J. Aoiz and L. Bañares, *J. Chem. Phys.* 2006, **125**, 094314.

[28] L. Bañares, F. J. Aoiz, P. Honvault, B. Bussery-Honvault and J.-M. Launay, *J. Chem. Phys.* 2003, **118**, 565-568.

[29] L. Bañares, F. J. Aoiz, P. Honvault and J.-M. Launay, *J. Phys. Chem. A* 2004, **108**, 1616-1628.

[30] K. J. Yuan, Y. Cheng, X. H. Liu, S. Harich, X. M. Yang and D. H. Zhang, *Phys. Rev. lett.*, 2006, **96**, 103202.

[31] H. Song, X. Y. Wang, R. T. Skodje and X. M. Yang, *Chin. J. Chem. Phys.*, 2006, **19**, 375-378.

[32] R. D. Levine, *Molecular reaction dynamics*, Cambridge University Press, Cambridge, 2005.

[33] C. F. Giese and W. R. Gentry, *Phys. Rev. A* 1974, **10**, 2156-2173.

[34] N. T. Goldberg, J. Y. Zhang, K. Koszinowski, F. Bouakline, S. C. Althorpe and R. N. Zare, *Proc. Natl. Acad. Sci. U.S.A.* 2008, **105**, 18194-18199.

[35] S. J. Greaves, E. Wrede, N. T. Goldberg, J. Y. Zhang, D. J. Miller and R. N. Zare, *Nature* 2008, **454**, 88-91.